Mycobiont contribution to tundra plant acquisition of permafrost-derived nitrogen

Rebecca E. Hewitt[1] (iD), M. Rae DeVan[2] (iD), Irina V. Lagutina[2] (iD), Helene Genet[3] (iD), A. David McGuire[3] (iD), D. Lee Taylor[2] (iD) and Michelle C. Mack[1] (iD)

[1]Center for Ecosystem Science and Society, Northern Arizona University, PO Box 5620, Flagstaff, AZ 86011, USA; [2]Department of Biology, MSC03 2020, University of New Mexico, Albuquerque, NM 87131, USA; [3]Institute of Arctic Biology, University of Alaska Fairbanks, PO Box 757000, Fairbanks, AK 99775, USA

Summary

• As Arctic soils warm, thawed permafrost releases nitrogen (N) that could stimulate plant productivity and thus offset soil carbon losses from tundra ecosystems. Although mycorrhizal fungi could facilitate plant access to permafrost-derived N, their exploration capacity beyond host plant root systems into deep, cold active layer soils adjacent to the permafrost table is unknown.

• We characterized root-associated fungi (RAF) that colonized ericoid (ERM) and ectomycorrhizal (ECM) shrub roots and occurred below the maximum rooting depth in permafrost thaw-front soil in tussock and shrub tundra communities. We explored the relationships between root and thaw front fungal composition and plant uptake of a ^{15}N tracer applied at the permafrost boundary.

• We show that ERM and ECM shrubs associate with RAF at the thaw front providing evidence for potential mycelial connectivity between roots and the permafrost boundary. Among shrubs and tundra communities, RAF connectivity to the thaw boundary was ubiquitous. The occurrence of particular RAF in both roots and thaw front soil was positively correlated with ^{15}N recovered in shrub biomass

• Taxon-specific RAF associations could be a mechanism for the vertical redistribution of deep, permafrost-derived nutrients, which may alleviate N limitation and stimulate productivity in warming tundra.

Introduction

Plant–mycorrhizal associations may control the potential for tundra vegetation to influence the regional carbon (C) balance of Arctic ecosystems. Both repeat photographic observations across the Arctic and experimental warming studies show the infilling of graminoid-dominated tundra by high productivity ectomycorrhizal (ECM) deciduous shrubs, along with the loss or stasis of evergreen ericoid mycorrhizal (ERM) shrub cover (Tape *et al.*, 2006; Myers-Smith *et al.*, 2011; Elmendorf *et al.*, 2012; Sistla *et al.*, 2013; Jorgenson *et al.*, 2015). These patterns of landscape greening may be associated with permafrost thaw (Martin *et al.*, 2017; Rocha *et al.*, 2018). Increases in plant productivity have the potential to offset C losses from degrading permafrost that underlies these ecosystems (Schuur *et al.*, 2008); yet, plant productivity is constrained by nutrient availability (Shaver *et al.*, 2001; Mack *et al.*, 2004; DeMarco *et al.*, 2014) and could be mediated by mycorrhizal access to thawed permafrost nutrients.

Globally, permafrost temperatures have increased and in the Northern Hemisphere have tracked increases in air temperature (Biskaborn *et al.*, 2019). On an annual timescale, with the progression of the growing season, the seasonally thawed portion of the soil profile – the active layer – deepens. Directional warming

and increased active layer thickness may therefore lead to thawing of transition layer and permafrost soils. Thawed permafrost soils undergo decomposition as they warm, releasing nitrogen (N) (Mack *et al.*, 2010; Keuper *et al.*, 2012; Salmon *et al.*, 2018), a primary limiting nutrient in tundra ecosystems (Shaver & Chapin, 1991; Chapin *et al.*, 1995). Recent studies suggest that nonmycorrhizal sedges and forbs with deep roots can access permafrost-derived N late in the growing season (Keuper *et al.*, 2017; Hewitt *et al.*, 2018; Blume-Werry *et al.*, 2019), stimulating productivity (Keuper *et al.*, 2017). However, the role of mycorrhizal fungi in controlling access to this novel nutrient source for shallowly rooted tundra shrubs is unknown. Tundra shrub access to deep nutrients could have a relatively high impact on regional C balance due to their higher growth potentials and longer tissue residence times than deeply rooted sedges and forbs.

Fungi are key to terrestrial nutrient cycling due to their impacts on decomposition, transformation of nutrient pools, and acquisition of nutrient sources to support their own production and, in the case of mycorrhizal fungi, that of host plants (Read & Perez-Moreno, 2003; Dighton, 2007; Hobbie & Horton, 2007; Phillips *et al.*, 2013). Of the mycorrhizal fungi, ERM and ECM fungi dominate high-latitude ecosystems (Read, 1991). Both ERM and ECM have saprotrophic capabilities to break down

complex nutrients along with the ability to use labile forms of nutrients (Bending & Read, 1996; Read, 1996; Read & Perez-Moreno, 2003), both of which are released from newly thawed permafrost (Mack *et al.*, 2010; Keuper *et al.*, 2012; Salmon *et al.*, 2018). Some ERM and ECM taxa are more adept at exploiting nutrient sources by increasing extramatrical mycelium density in nutrient-rich patches (Bending & Read, 1995; Dickie *et al.*, 1998; Tibbett, 2000; Smith & Read, 2008). Besides ERM and ECM, other root-associated fungi (RAF) such as dark septate endophytes (DSE) have been implicated in plant nutrient uptake (Newsham *et al.*, 2009; Newsham, 2011) albeit by poorly understood physiological mechanisms. Together this suggests that RAF are the gatekeepers of plant nutrient acquisition for many tundra plants.

The exploration capacity of RAF beyond the root system of host plants into deep, cold active layer soils adjacent to the permafrost table is unknown. Few studies describe fungal distributions throughout the full active layer (but see Penton *et al.*, 2013) or at taxonomic resolutions that support ecological inferences. However, many authors have suggested that ERM are important only in surficial organic horizons due to shallow root proliferation of their plant hosts (see references in Read, 1991) and the limited extension of ERM hyphae beyond colonized roots (Read, 1991; Grelet *et al.*, 2010). By contrast, a number of ECM taxa can extend the foraging reach of root systems in the form of extramatrical mycelium (Agerer, 2001; Weigt *et al.*, 2012) that can grow tens of meters (Dahlberg & Stenlid, 1990; Bonello *et al.*, 1998; Bergemann & Miller, 2002). Thus, ECM hosts should have a greater capacity to access soil resources far below the rooting zone, such as recently thawed permafrost-derived N, than would co-occurring ERM hosts by virtue of their fungal traits.

The aim of our study was to investigate whether RAF contribute to shrub access to newly-thawed permafrost N. We first determined whether RAF mycobionts were present and active at the permafrost thaw front beyond host plant root systems. We then sampled mycorrhizas of ERM and ECM host plants and compared these root tip fungal communities to fungal RNA and DNA profiles from the permafrost thaw front. We tested for correlations between the degree of host plant RAF connection to the thaw front and acquisition of a deeply applied ^{15}N tracer in tussock and shrub tundra that represent communities on the spectrum of anticipated vegetation change across the Arctic (Myers-Smith *et al.*, 2011). Specifically, we asked the following questions:
(**1**) Do some host plants or tundra vegetation communities have greater root-associated fungal connectivity to the thaw front?
(**2**) Are connections between root-associated fungi and the thaw front related to the supply of deep N to plant tissues?
(**3**) Does the composition of fungi at the thaw front suggest a large active soil community engaged in N acquisition that could facilitate vertical transfer to host plants?
(**4**) What vegetation and edaphic factors influence the composition of root-associated fungi that may connect host plants to the thaw front?

To our knowledge, this investigation provides the first observations of root-associated fungal connectivity to the thaw front and contribution to plant acquisition of deep N offering insights into how fungal communities may mediate ecosystem responses to the release of permafrost-derived N.

Materials and Methods

Study site

The experiment was conducted in sub-arctic tundra near Eight Mile Lake (63°52′42″N, 149°15′12″W), AK, USA, where permafrost, vegetation and ecosystem carbon balance are well-studied (Schuur *et al.*, 2007; Vogel *et al.*, 2009; Mauritz *et al.*, 2017). The surface permafrost is relatively warm (−1.0°C) and thus vulnerable to thaw (Osterkamp & Romanovsky, 1999). Maximum thaw depth has increased by 2.1 cm yr^{-1} due to surface permafrost degradation (Plaza *et al.*, 2019), and newly thawed permafrost soils have greater inorganic nitrogen (N) content than active layer soils (Salmon *et al.*, 2018) near the study site. The vegetation is classified as moist acidic tundra and is composed of deeply rooted, nonmycorrhizal graminoids and forbs, and moderately rooted deciduous and evergreen ectomycorrhizal (ECM) and ericoid mycorrhizal (ERM) shrubs (Table 1; Hewitt *et al.*, 2018). Within the graminoid-dominated tussock tundra there are patches of shrub tundra dominated by *Betula nana* L.

Isotope tracer addition and plant harvest

To investigate the ability of tundra shrubs to immediately access permafrost-derived N, a deep ^{15}N isotope tracer was applied at the end of the growing season when active layer thickness was close to its maximum (Hewitt *et al.*, 2018). At the time of labeling, the mean thaw depth measured in the experimental plots was 61.2 cm ± 4.8 SE. In brief, 10×1 m^2 plots (tussock $n = 5$ and shrub $n = 5$) were labeled with 98 atom% ammonium chloride applied at nine injection points at the permafrost table using long stainless steel needles to achieve an addition of 250 mg of ^{15}N m^{-2} matching the composition and pool size of newly thawed N at this site (Salmon *et al.*, 2018, Supporting Information Methods S1). Twenty-four hours after isotope addition, above- and belowground plant biomass was harvested to determine uptake of the tracer. Belowground plant biomass and soils were collected at 10-cm depth increments down to the permafrost boundary with the exception of the top 0–5 cm of the soil profile. Live roots and rhizomes were removed from organic and mineral soils at each depth increment by hand and cleaned with nanopure water. Root species identities were verified using plant internal transcribed spacer (ITS) restriction fragment length polymorphism analysis and used to correct fine-root species identity, biomass and isotope signature (Hewitt *et al.* 2018). Root fungal communities were characterized from these root samples (Methods S1).

Thaw front fungi sampling

To characterize the thaw front fungal community below the maximum rooting depth of mycorrhizal shrubs, we cored the 10 cm of thawed soil above the permafrost table (*c.* 69 cm in tussock and *c.* 48 cm in shrub at top of core) for fungal RNA and DNA

Table 1 Characteristics of ectomycorrhizal and ericoid mycorrhizal host plants in tussock and shrub tundra at Eight Mile Lake, AK, USA.

Species	Mycorrhizal guild	Maximum rooting depth (cm)		Max root: thaw depth		Fine-root biomass (g m^{-2})		Percentage tracer recovered in total biomass	
		Tussock	Shrub	Tussock	Shrub	Tussock	Shrub	Tussock	Shrub
Rhododendron tomentosum	ERM	41.40 ± 8.03	34.8 ± 5.60	0.54 ± 0.11	0.60 ± 0.09	133.56 ± 27.56	273.86 ± 86.96	0.06 ± 0.05	0.014 ± 0.004
Vaccinium uliginosum	ERM	42.00 ± 11.61	30.25 ± 4.21	0.55 ± 0.16	0.54 ± 0.09	62.32 ± 23.91	66.51 ± 36.48	1.337 ± 1.31	0.001 ± 0.001
Vaccinium vitis-idaea	ERM	35.75 ± 6.98	25.8 ± 5.52	0.48 ± 0.09	0.46 ± 0.11	14.80 ± 6.57	30.52 ± 12.51	0.186 ± 0.15	0.004 ± 0.002
Empetrum nigrum	ERM	18 ± 13	23 ± 1	0.19 ± 0.12	0.40 ± 0.01	3.27 ± 2.08	48.19 ± 44.52	0.002 ± 0.002	0.001 ± 0.001
Betula nana	ECM	30.50 ± 6.66	26.8 ± 4.53	0.40 ± 0.10	0.47 ± 0.09	45.38 ± 12.08	290.05 ± 118.34	0.003 ± 0.003	0.016 ± 0.009

Values represent plot means ± SE (tussock n = 5, shrub n = 5). Rooting depth and biomass values acquired from Hewitt *et al.* (2018). ECM, ectomycorrhizal; ERM, ericoid mycorrhizal.

analysis. We split the 10 cm core into four depth segments using a sterile knife and sampled *c.* 2 g of soil from the center of each segment directly into a MoBio RNeasy PowerSoil bead tube (Qiagen Inc., Valencia, CA, USA), and immediately placed the samples in liquid N.

Soil chemistry

For each soil depth increment we measured: (1) pH of air-dried samples mixed in a 1 : 5 (organic) or 1 : 1 (mineral) solution with nanopure water using a SymPHony pH Meter (VWR, Radnor, PA, USA); (2) C and N concentrations of bulk soil dried at 60°C for 48 h, ground and run on an Elemental Analysis-Isotope Ratio Mass Spectrometer (Delta Advantage, Thermo Fisher Scientific, Waltham, MA, USA) coupled to an Elemental Combustion Analyzer (ECS4010, Costech, Valencia, CA, USA); (3) total N, nitrate (NO_3-N), ammonium (NH_4-N), and dissolved organic C (DOC) on ~ 35 g soil extracted in 0.1M K_2SO_4, filtered through GF/A filters, measured on a TOC-L (DOC and total N, Shimadzu Corp., Kyoto, Japan) and a Smart Chem 200 (NO_3-N and NH_4-N, Unity Scientific, Brookfield, CT, USA), and expressed in relation to oven-dry equivalent. Soil depth increments were matched with the closest root-depth increment for further analysis.

Root and thaw front fungal composition

Genomic DNAs from clean root samples were isolated with the DNEasy Plant Mini Kit (Qiagen). Thaw-front fungal RNA and DNA were isolated with the MoBio RNeasy PowerSoil kit (Qiagen) with the DNA elution kit according to the manufacturer's protocol. Complementary DNA (cDNA) was synthesized from the isolated RNA using reverse transcription. The fungal ITS2 region from root DNA and soil DNA and cDNA were amplified and sequenced using ITS4-Fun and 5.8S_Fun (Taylor *et al.*, 2016) on the Illumina MiSeq platform. Resulting sequences were demultiplexed, quality-filtered and mapped to operational taxonomic units (OTUs, GenBank accession no. MN151409-MN152926; Table S1) at 97% similarity using the UPARSE pipeline in Usearch v.10.0.240 (Edgar, 2013). Taxonomy was assigned using the RDP and Warcup ITS databases (Despande *et al.*, 2016) and supplemented with manual assignments based on NCBI Blastn and placement in maximum-likelihood trees (Fig. S1). Guilds were assigned using a combination of FUNguild (Nguyen *et al.*, 2016) and investigator knowledge. Root fungal communities were pooled by host species × depth increment after sequencing. Thaw-front fungal samples were analyzed in two ways: (1) separately for community analyses and (2) the four depth samples from each 10-cm thaw-front core were pooled after sequencing for analyses comparing thaw front and root fungi and plant metrics (Methods S1).

Subsets of fungal communities

Our fungal data were derived from three sources (roots, thaw-front soil DNA and thaw-front soil RNA) and assigned to

community subsets (Table S2; Fig. S2). First, we described the total thaw front community (TOT$_{TF}$), which we subset into putatively active (ACT$_{TF}$) and dormant (DOR$_{TF}$) components (Table S2; Fig. S2). The ACT$_{TF}$ contains OTUs observed in thaw-front RNA, thaw front-RNA and DNA, or thaw-front DNA also in root-tip mycorrhiza communities. The ACT$_{TF}$ is the fungal community that has the potential to acquire permafrost-derived N, whereas the DOR$_{TF}$ component, which was observed only in thaw-front DNA, is likely not involved. We assumed that all taxa detected on roots were active (ACT$_R$), because spores and ancient DNA are not expected to have appreciable abundances on clean, actively growing roots. From the active fungi at the thaw front and on roots (ACT$_{TF}$ and ACT$_R$), which encompasses fungi of many guilds, the root-associated fungi (RAF$_{TF}$ and RAF$_R$) were derived as OTUs with guild or taxonomic identities that infer mycorrhizal function (Table S2; Fig. S2). When an OTU in the RAF$_{TF}$ and RAF$_R$ was observed in the same plot, it was determined to be a RAF taxon that may potentially connect root systems to the thaw front, referred to as RAF connector taxa (CON$_{TF}$ and CON$_R$) (Table S2; Fig. S2). Subsequent analyses were conducted on each community subset.

Statistical analyses

We calculated a fungal connectivity index that represents the degree to which taxa on root systems of a given host plant at each depth increment also were represented at or 'connected' to the thaw front (CON$_R$ and CON$_{TF}$). Due to inadequate recovery of RNA from the thaw front, a combination of RNA and DNA OTUs were used for connectivity calculations (CON$_{TF}$), and derived from the active fungi observed at the thaw front (ATC$_{TF}$) (Table S2; Fig. S2), a decision validated with a sensitivity analysis comparing RNA and ATC$_{TF}$ profiles (Methods S1). The connectivity index was calculated from the CON community subset as the relative abundance of a given OTU in a root sample (CON$_R$) multiplied by the relative abundance of that OTU at the thaw front (CON$_{TF}$) of the same plot. In addition to the OTU-level connectivity indices, we attained an overall connectivity index for each host plant × depth by summing the connectivity metric of all OTUs, and we further summed this at the host plant × plot level (Methods S1). We tested for relationships between OTU-specific and the summed connectivity indices and plant metrics.

All analyses were completed in R 3.5.2 (R Core Team, 2018). For all analyses, the OTU table was relativized in the PHYLOSEQ package (McMurdie & Holmes, 2013) by community subset depending on the research question at hand (Methods S1).

Variation in RAF connectivity to the thaw front and N uptake

We built candidate linear mixed effects models with the package R/NLME (Pinheiro et al., 2017) to test whether the fungal connectivity index, representing potential connection between fine roots and the thaw front, was related to each fixed factor

that represented a hypothetical driver of connectivity: host-plant species, tundra community, fine-root biomass (g m^{-2}) and the ratio of root: thaw depth. Here, each sample represented host plant × depth increment. Plot was included as a random factor to account for spatial differences and the correlation structure of an autocorrelation moving-average model (i.e. corARMA, Zuur et al., 2009) was implemented to account for nonindependence among root samples within plots. Connectivity was rank-transformed to meet assumptions of homoscedasticity and normality. For each candidate model, we calculated AICc (sample size corrected Akaike Information Criterion) and ranked model Akaike weights with the AICMODAVG package (Mazerolle, 2019). We computed model-averaged estimates to assess the significance of the fixed factors (Burnham & Anderson, 2002).

We tested whether fungal connectivity to the thaw front was related to the supply of deep N to plant tissues. First, we used a logistic mixed effects model to explore whether the fixed factor of summed connectivity index (host plant × depth) was related to the acquisition of isotope (y/n) with plot as the random factor using the LME4 package (Bates et al., 2015). We also assessed covariation in isotope concentration, atom percent excess (APE), and pool size (g ^{15}N m^{-2}) in fine root samples in relation to the summed connectivity index by fitting linear mixed effects models using the NLME package. We resorted to ranking APE and pool size to meet model assumptions. First, we tested whether variation in isotope metrics were a function of the fixed factors connectivity × host plant species and connectivity × tundra community. Neither interactions were significant; therefore, the final models tested were ranked fine root APE or pool size as a function of the fixed factors connectivity, host plant, and tundra community with plot as a random factor and a corARMA structure. Because our interest was in the effect of connectivity on the isotope in fine root samples, we tested model significance by evaluating the log likelihood ratio (L ratio) of our final model in comparison to the model with the fixed factors host plant and tundra community. We also tested whether taxon-specific connectivity covaried with deep N access. Diagnostic plots indicated a high level of skew in both the isotope and OTU-level connectivity, which did not improve with transformations or adjustments to model-specified data distributions. As such, we calculated Spearman correlation coefficients between the OTU-level connectivity index and the pool of isotope in each fine root sample.

We also explored how connectivity related to the overall acquisition of deep N within 24 h. We summed both fungal connectivity and aboveground and belowground percent tracer recovered by host plant × plot. Host plant × plot estimates of tracer recovery were summed from aboveground harvest tissues and rhizomes and belowground harvest root samples. We modeled the ranked percent isotope recovery in relation to the fixed factor connectivity with plot as a random factor using the same model evaluation steps described above. Again, we computed Spearman correlation coefficients between the OTU-level connectivity index and percent tracer recovered by each host plant to evaluate taxon-specific effects on total deep N access.

Table 2 Ranked candidate model comparison of plant metrics explaining variation in fungal connectivity between root systems and the thaw front at Eight Mile Lake, AK, USA.

Model	Variable	K	AICc	Δ AICc	AICc w_i	Log L	R_m^2	R_c^2
M1	Root: thaw depth	5	660.12	0	0.66	−324.66	0.02	0.79
M2	Fine-root biomass (g m^{-2})	5	663.29	3.16	0.14	−326.24	0.02	0.77
Null	None	4	664.55	4.42	0.07	−328.01	0	0.76
Full	M1 + M2 + M3 + M4	11	664.95	4.83	0.06	−319.56	0.15	0.81
M3	Tundra community	5	665.38	5.25	0.05	−327.29	0.11	0.76
M4	Host plant	8	667.17	7.04	0.02	−324.58	0.02	0.79

Candidate model attributes include the number of parameters (K), the sample size corrected Akaike information criterion (AICc), the change in AICc relative to the best model (ΔAICc), the AICc-based model weight (AICc w_i), the Log-likelihood (Log L), the marginal R^2 accounting for fixed effects only (R_m^2), and the conditional R^2 accounting for both fixed and random effects (R_c^2). M1 was assessed as the best model of the suite of models tested based on AICc; however, model-averaged parameter estimates of the root: thaw depth indicate that this, the best parameter and candidate model, was not a significant predictor of variation in RAF connectivity.

Characterization of thaw front and root fungal communities

We tested whether fungal composition at the permafrost boundary suggests a large active community with the potential to transfer N vertically to host plants. We first characterized the dormant (DOR_{TF}) and active (ACT_{TF}) thaw front communities and compared the root-associated fungi at the thaw front (RAF_{TF}) to taxa observed on roots (RAF_R). We evaluated variation in composition of root and thaw front root-associated fungi (RAF_{TF} and RAF_R) and potential connector taxa (CON_{TF} and CON_R) among host plant species and tussock and shrub tundra communities using nonmetric multidimensional scaling (NMDS) ordinations (Kruskal, 1964) with the R/VEGAN package (Oksanen et al., 2012). We determined which environmental variables were correlated (P < 0.05) with variation in connector taxa (CON_{TF} and CON_R) composition. We used permutational multivariate analysis of variance to make comparisons between fungal communities associated with tundra communities (ACT_{TF}, RAF_{TF}, RAF_R, CON_R) and host plants (RAF_R, CON_R) in the R/VEGAN package. We used indicator species analysis of OTUs that comprised at least 1% of the total fungi by relative abundance to test whether the relative abundance of each OTU indicated a significant association with host plant and/or tundra community for root and thaw front community subsets (ACT_{TF}, RAF_R, CON_R) with the R/INDICSPECIES package (De Caceres & Legendre, 2009).

Results

### Does RAF connectivity vary by host and tundra community?

Neither host species nor tundra community were strong explanatory variables of the degree of RAF connectivity (Table 2; Fig. 1). The best models explaining variation in RAF connectivity included root: thaw depth followed by fine-root biomass (Table 2). However, the model-averaged parameter estimates for these top fixed factors lacked significant explanatory power (Fig. S3a,b, root: thaw depth est$_{(n=81)}$ = 2.19, 95% CI = −1.07, 5.44; fine-root biomass est$_{(n=81)}$ = 0.64, 95% CI −2.15, 3.44), suggesting that overall connectivity to the thaw front is ubiquitous regardless of root traits, host or tundra community in our study system.

Is RAF connectivity linked to plant access to newly thawed permafrost-derived N?

RAF connectivity and fine-root isotope uptake The magnitude of RAF connectivity did not predict the presence of deeply applied ^{15}N isotope in a fine-root sample (z-value$_{(n=81)}$ = −1.25, $P = 0.21$). When we assessed continuous variation in enrichment, the overall RAF connectivity again explained neither variation in APE (L ratio$_{(n=81)}$ = 1.59, $P = 0.21$) nor the pool of isotope (L ratio$_{(n=81)}$ = 1.29, $P = 0.26$) in fine-root samples, supporting the logistic model results.

We observed 16 OTUs with significant positive ($n = 8$) or negative ($n = 8$) correlations between isotope pool size and the OTU-level connectivity index (Fig. 2a; Table S3). The connectivities of five ascomycetes, all in the Helotiaceae, and three basidiomycetes, were positively correlated with tracer pool size in fine-
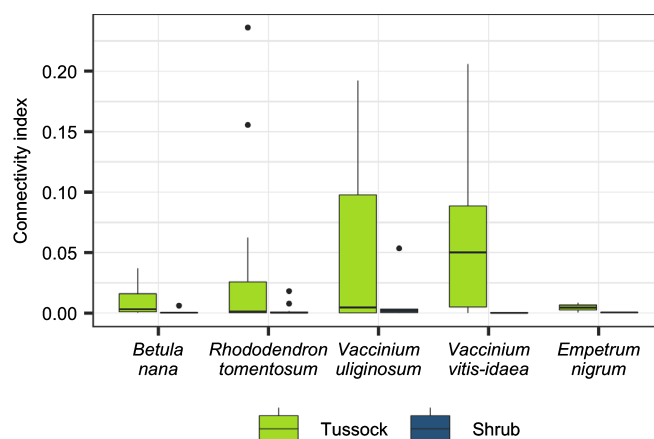
Fig. 1 Fungal connectivity of putatively root-associated fungi between roots and the thaw front environment for each host species in tussock and shrub tundra. Boxplot represents the connectivity index for fine-root samples at each depth increment among plots. The lower and upper bounds of the boxplot show the first and third quartiles (the 25th and 75th percentiles), the middle line shows the median, whiskers above and below the boxplot indicate 1.5 × inter-quartile range, and points beyond the whiskers indicate outlying points.

(a)

(b)
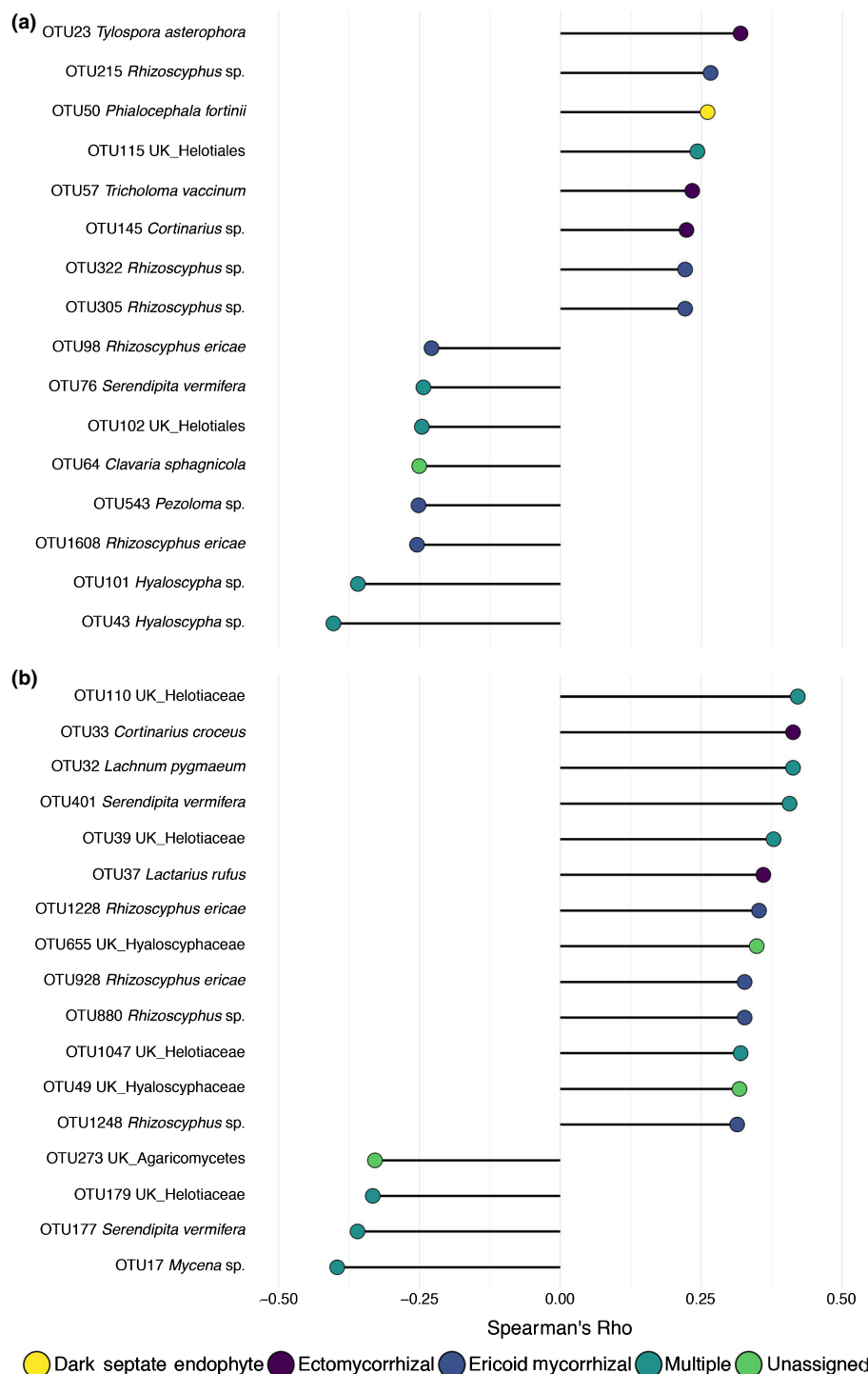
Fig. 2 Spearman's rank correlation coefficients for operational taxonomic units with significant correlations between (a) tracer pool (g ^{15}N m^{-2}) of fine-root samples and summed connectivity index to the thaw front (host plant × depth), and (b) overall percentage of tracer recovered in above- and belowground plant tissues and summed connectivity index to the thaw front (host plant × plot).

root samples. *Tylospora asterophora* showed the strongest positive correlation, whereas *Hyaloscypha* sp. showed the strongest negative correlation.

RAF connectivity and total isotope recovery Average percentage tracer recovery in live plant biomass was low but detectable, ranging from 0.001% ± 0.0009 to 1.33% ± 1.31. Overall, there was a tendency for greater RAF connectivity to result in a modest increase in percentage tracer recovered (L ratio$_{(n=50)}$ = 3.13, P = 0.08) in plant tissues. Isotope recovery and fungal

connectivity was highest for *V. uliginosum* in tussock tundra, but this relationship was not different between species or tundra community (Fig. 3). Our analysis revealed taxon-specific relationships between the OTU-connectivity index and the total percentage tracer recovered (Fig. 2b; Table S3). Ascomycetes in the Helotiales showed significant positive and negative correlations with total percentage isotope recovered in plant tissue. Of the Basidiomycota, the genera *Cortinarius*, *Lactarius* and *Serendipita* showed positive correlations, whereas another *Serendipita*, *Mycena*, and an unknown Agaricomycete showed negative
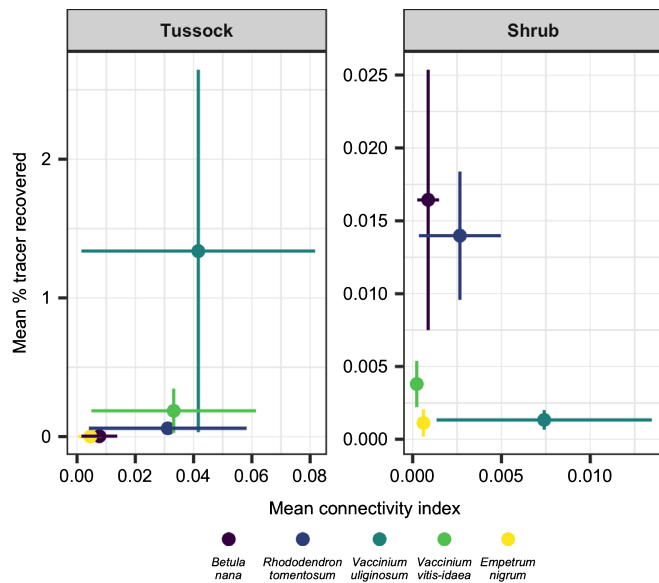
Fig. 3 Mean percentage isotope recovered in above- and belowground plant tissues in relation to the summed connectivity (host plant × plot) of root-associated fungi to the thaw front. Points represent means with SE. Note different *y*-axes.

correlations between the connectivity index and percentage tracer recovered. The majority of fungi that were significantly correlated with isotope recovery in total plant biomass were helotialian fungi (Fig. 2b; Table S3).

Characterization of thaw front and root fungal communities

Our sequencing effort yielded > 19 million sequences from the thaw front and > 10 million from root tips. These DNA (root and soil) and RNA (soil) sequences were grouped into 1518 OTUs (TOT_{TF} + ACT_R). Root DNA sequences (ACT_R) yielded 1117 OTUs, and soil RNA and DNA sequences yielded 701 (TOT_{TF}); 300 OTUs were found in both root and soil datasets (Table S1). The active (ACT_{TF} + ACT_R) fungal community consisted of 1367 OTUs. Of these, 250 OTUs were unique to the soil thaw front (i.e. not observed on roots) as either DNA or RNA, and 817 were unique to root communities (i.e. not observed in the soil). In the ACT species pool, 300 (i.e. 22%) were categorized as RAF. Finally, 55% of the RAF showed evidence of connection between roots and soil, yielding 164 OTUs in the CON community.

Thaw-front fungi

The dormant thaw-front community (DOR_{TF} $n = 151$) represented only 0.05% of the total fungal reads, the majority of which were either unassigned to a guild or assigned to multiple guilds due to coarse taxonomic placement or poorly understood ecologies (Table 3a,b).

The ACT_{TF} community was composed of 550 OTUs, of which the majority belonged to the Ascomycota, with the Basidiomycota a distant second, and the Mucoromycota represented a very small proportion (Table 3a). By relative abundance, the

largest fraction of OTUs were assigned to multiple guilds followed by ERM, ECM or saprotroph guilds (Table 3b). Taxa assigned to other guilds accounted for < 5% of the ACT_{TF} community. Helotiaceae sp. (OTU 1) was by far the most abundant taxon (~25.52% relative abundance) followed by *Pezoloma* sp. (OTU 2) and *Rhizoscyphus ericae* (OTU 3) which each made up ≥ 5% of the ACT_{TF} community and thus indicated high relative abundance of ERM in these deep, cold soils (Table 3b; Fig. 4a).

The ACT_{TF} composition differed between tussock and shrub communities ($R^2_{(n=69)} = 0.23$, $P < 0.01$). Of 63 indicator taxa in the tussock community, the majority were assigned to multiple guilds or were RAF identified as ERM, ECM or dark septate endophytes (DSE) (Table S1). Thirty-six of the tussock indicator taxa also were observed on roots. *Rhizoscyphus ericae* (OTU 98), was the strongest indicator (IndVal = 0.925, $P < 0.001$) and had the highest abundance of all indicator taxa that were found both at the thaw front (*c.* 8.63% relative abundance) and on roots (*c.* 10.19%) in tussock vegetation. Comparatively, there were only nine indicator taxa at the shrub tundra thaw front (Table S1), four of which also were found in the root community: *Rhizoscyphus* sp. (OTU 25), *Lachnum pygmaeum* (OTU 32) and Helotiaceae sp. (OTUs 31, 115). Following compositional patterns of the ACT_{TF}, the thaw-front root-associated fungi (RAF_{TF} $n = 268$) also differed by tundra community (Fig. S4; $R^2_{(n=81)} = 0.17$, $P < 0.001$).

Root-tip fungi

The sequence dataset from live roots (ACT_R) yielded 1117 OTUs predominantly in the Ascomycota, secondarily in the Basidiomycota, and few taxa with low abundance in the Mucoromycota (Table 3a). There were 102 families and 149 genera. Several of the most abundant OTUs were ERM and ECM taxa (Fig. 4a). We observed that many taxa were assigned to non-RAF or multiple guilds; however, of the taxa that could be assigned to one guild, the majority were RAF (Table 3b).

Of the 1117 OTUs in ACT_R, 379 were considered RAF_R (Fig. 4a) and followed the same abundance trends at the phylum scale as the ACT_R community (Table 3a). Of the 379 RAF_R taxa, ~ 43% were assigned to one guild and a quarter were assigned to multiple guilds or unassigned but classified as RAF due to taxonomic affinities to a RAF guild. The composition of the RAF_R varied with tundra community (Fig. S4; $R^2_{(n=81)} = 0.05$, $P < 0.001$) and host plant ($R^2_{(n=81)} = 0.15$, $P < 0.001$). There were 13 indicator taxa of tussock tundra and 21 of shrub tundra in the guilds ECM, ERM, multiple guilds and unassigned guilds (Table S1). Nine of the tussock and seven of the shrub indicator taxa also were observed at the thaw front (RAF_{TF}; Table S1). *Empetrum nigrum* was the only host with a RAF indicator taxon, *Pezoloma* sp. (OTU702), that also was observed at the thaw front (Table S1). Several RAF taxa showed significant associations with groups of host plants (Table S1).

Connectivity between the thaw-front and root systems

Of the 300 RAF taxa that occurred in both root and thaw-front profiles (RAF_R + RAF_{TF}), 164 occurred in the same plots and thus

Table 3 Counts and taxonomic relative abundances for (a) phyla and (b) guilds for each community subset observed on root tips and at the permafrost thaw front at Eight Mile Lake, AK, USA.

(a)

Community	Phylum	No. of OTUs	Relative abundance, RA (%)	
Dormant thaw front	Ascomycota	91	75.8	*
$n = 151$ OTUs	Basidiomycota	58	24.09	*
	Mucoromycota	2	0.11	*
Active thaw front	Ascomycota	372	81.22	●
$n = 550$ OTUs	Basidiomycota	163	17.39	●
	Mucoromycota	15	1.39	● ●
Active root tip	Ascomycota	769	75.48	◊
$n = 1117$ OTUs	Basidiomycota	315	24.33	◊
	Glomeromycota	1	1.01E-05	◊
	Mucoromycota	32	0.18	◊ ◊ ◊
Root-associated fungal connectors	Ascomycota	118	67.96 (root tip)	+
$n = 164$ OTUs			84.48 (thaw front)	+
	Basidiomycota	46	32.04 (root tip)	+
			15.52 (thaw front)	+

(b)

Guild	Dormant thaw front $n = 151$ OTUs		ACT thaw front $n = 550$ OTUs		ACT root tip $n = 1117$ OTUs		RAF connectors $n = 164$ OTUs		
	No. of OTUs	Relative abundance (%)[*]	No. of OTUs	Relative abundance (%)•	No. of OTUs	Relative abundance (%)◊	No. of OTUs	Relative abundance roots (%)[+]	Relative abundance thaw front (%)[+]
Animal endosymbiont	5	5.77	10	4.25	12	0.14			
Animal pathogen			1	0.03	3	8.20E-04			
AM					1	1.00E-04			
DSE	1	0.04	17	3.01	17	2.8	8	4.46	7.73
ECM	27	8.79	60	10.98	80	13.43	36	19.72	19.36
ERM	5	0.71	60	21.74	66	23.9	46	35.49	40.99
Fungal parasite	1	2.26	1	2.00E-05	3	6.80E-03			
Lichenized	7	2.89	7	0.13	14	0.18			
Lichenicolous			2	0.25	2	11.82			
Multiple	24	11	157	45.07	302	29.43	55	36.36	31.4
Bryophilous					1	1.30E-04			
Plant pathogen	14	12.02	13	0.16	29	0.43			
Saprotroph	25	16.05	63	8.12	151	11.77			
Unassigned	42	40.47	159	6.26	436	6.09	19	3.96	0.52

AM, arbuscular mycorrhizal; DSE, dark septate endophyte; ECM, ectomycorrhizal; ERM, ericoid mycorrhizal; ACT, active; RAF, root-associated fungi. Connectors were observed on roots and at the thaw front in the same profile.
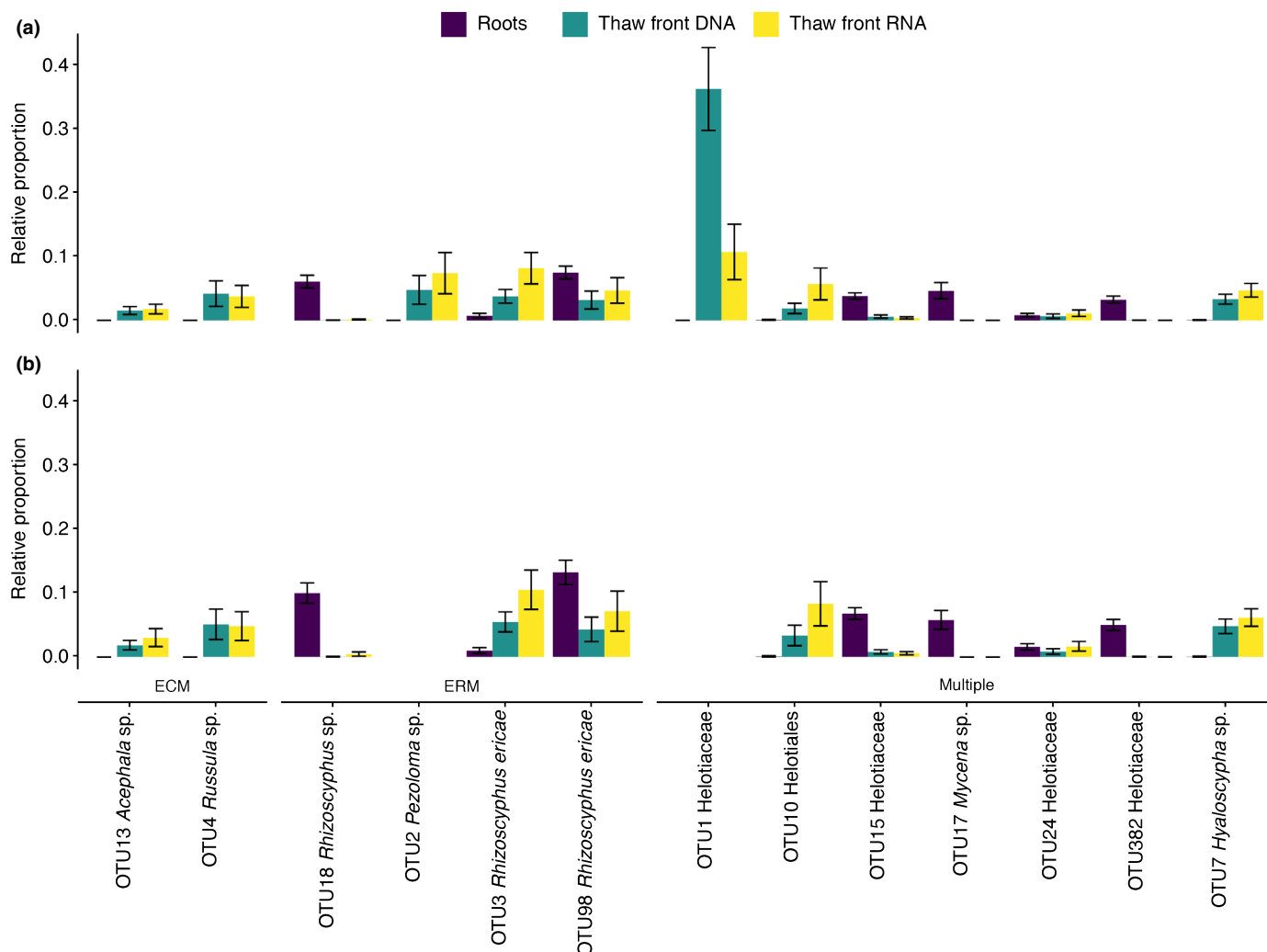*, RA out of 151 operational taxonomic units (OTUs).
•, RA out of 550 OTUs.
◊, RA out of 1117 OTUs.
+, RA out of 164 OTUs.

were considered potential connector taxa between the thaw-front and root systems (Figs 4b, 5). In the connector community (CON$_R$ and CON$_{TF}$), there were two phyla, 19 families, 28 genera and 50 species assigned to multiple guilds, ERM, ECM, DSE and unassigned (Table 3a,b). Surprisingly, the taxonomic identities of the top most-connected taxa show the potential importance of ERM and DSE in addition to ECM in connecting plant roots to permafrost resources (Fig. 6a,b). The most abundant CON$_R$ taxa were *Rhizoscyphus ericae* (OTUs 98, 3), Helotiaceae sp. (OTU 15), and Helotiales sp. (OTU 24), emphasizing the importance of ERM in potential access to the permafrost boundary.

The connector community observed on roots (CON$_R$) had compositional differences between host plants ($R^2_{(n=81)} = 0.16$, $P < 0.01$) and tundra communities ($R^2_{(n=81)} = 0.05$, $P < 0.01$; Fig. 7a). Ten taxa were indicators of shrub tundra: *Rhizoscyphus* (OTUs 127, 215, 242 and 662), *Lactarius rufus* (OTU 37), *Mycena* sp. (OTU 58), *Serendipita vermifera* (OTU 174) and several poorly identified Hyaloscyphaceae sp. (OTUs 49, 59, 337; Table S1). Tussock tundra had nine indicator taxa: *Rhizoscyphus* (OTUs 1608, 1265), *Pezoloma* (OTU 702), along with *Russula nitida* (OTU 41), *Meliniomyces variabilis* (OTU 709), *Serendipita vermifera* (OTUs 129), *Thelephora terrestris* (OTU

Fig. 4 Fungal taxonomic relative abundances from thaw-front and root communities. The operational taxonomic units (OTUs) shown include the 10 most abundant OTUs from each of the following groups: (a) putatively root-associated fungi at the thaw front and on roots (RAF_{TF} and RAF_R) and (b) potential root-associated connector fungi at the thaw front and on roots (CON_{TF} and CON_R). The relative abundances shown on the *y*-axis of panel (a) were relativized by the active fungal community (ACT_{TF} and ACT_R), and panel (b) by the root-associated community (RAF_{TF} and RAF_R). SE computed based on relative abundances in each of the 69 soil samples and 81 root samples. Fungal guild: ECM, ectomycorrhizal; ERM, ericoid mycorrhizal; and Multiple guilds.

106) and Helotiales (OTUs 216, 110; Table S1). Individual host plants did not have significant associations with particular CON_R taxa. However, the ERM hosts together had five indicator taxa that also were observed at the thaw front (Table S1): *Clavaria sphagnicola* (OTU 64), *Rhizoscyphus ericae* (OTUs 912, 1608), *Serendipita vermifera* (OTU 76) and an unknown Helotiaceae (OTU 102). The CON community, as a whole, accounted for 71% of the RAF ($RAF_R + RAF_{TF}$) by relative abundance, suggesting a large active community that may facilitate the vertical transfer of thawed permafrost N. Individual taxa within the $CON_R + CON_{TF}$ community occurred in 0.6% to 88% of the samples.

We observed correlations ($P < 0.05$) between the composition of connector taxa observed on roots (CON_R) and bulk soil %N, bulk soil C : N, and extractable dissolved inorganic N (μg $NO_3 + NH_4 \ ODE^{-1}$; Fig. 7a; Table S4). In contrast, thaw depth was the only variable correlated with the composition of the

connector taxa observed at the thaw front (CON_{TF}; Fig. 7b; Table S4).

Discussion

Overview

Our previous research showed that only nonmycorrhizal plants extend their roots to the thaw front (Hewitt *et al.*, 2018), posing a conundrum. Why would mycorrhizal plants forgo the opportunity to acquire limiting nutrients that are relatively abundant close to the permafrost? Here we show that all ERM and ECM host plants examined were associated with mycobionts that occurred in an active state at the permafrost thaw front. To our knowledge, this is the first evidence that ECM and ERM host plants have access to N in the region of thawing permafrost through their mycobionts. Furthermore, we found that plant
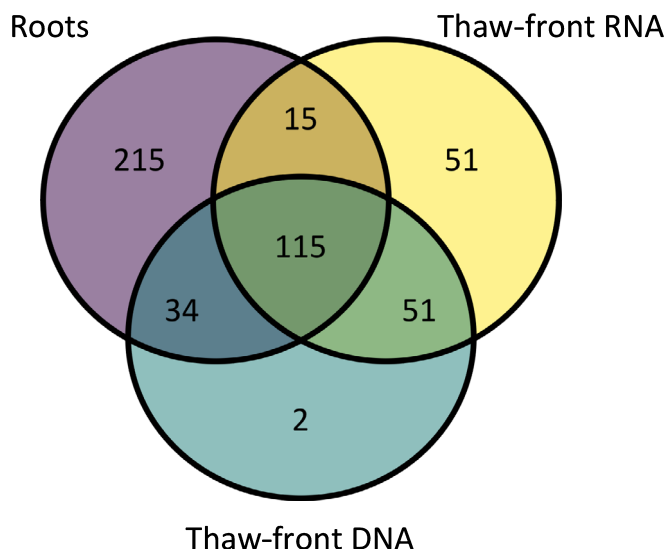
Fig. 5 Venn diagram showing richness of putatively root-associated fungi observed at the thaw front and on roots (RAF$_{TF}$ and RAF$_R$). Taxa reported from DNA profiles of roots and DNA and RNA profiles of thaw front soils, excluding putatively dormant operational taxonomic units that occur only in soil DNA (DOR$_{TF}$). Shared taxa may provide connectivity between shallow root systems and the deeper, permafrost thaw boundary.

uptake of thaw front N was correlated with specific root-associated fungi.

Fungal composition

Our observations of fungal composition throughout the active layer support previous investigations in surface soils where vegetation community (tussock vs shrub) was a strong driver of microbial composition (Wallenstein *et al.*, 2007). Previous reports of root-associated fungi (RAF) for tundra ECM and ERM hosts also corroborate our observation of abundant taxa in the genera *Rhizoscyphus*, *Mycena*, *Russula*, *Lactarius*, *Meliniomyces*, *Cortinarius*, *Phialocephala*, *Hyaloscypha* and *Leccinum* (Walker *et al.*, 2011; Timling & Taylor, 2012). We provide additional support for the view that RAF are predominantly generalists among co-occurring ERM (Walker *et al.*, 2011) and ECM hosts (Timling *et al.*, 2012). For example, we observed few fungal indicator species for individual plant hosts and abundant taxa among multiple hosts.

In a strongly N-limited system such as tundra (Schimel *et al.*, 1996; Mack *et al.*, 2004), we would anticipate that RAF may have greater ability to acquire N from newly thawed permafrost due to less carbon (C) limitation compared to saprotrophs (Hogberg *et al.*, 2007). Of the active thaw front (ACT$_{TF}$) taxa that could be identified to a single guild, most were RAF, followed by saprotrophic fungi. However, we could not assign most taxa at the thaw front to a single guild, in part due to poor taxonomic identification and/or understanding of their ecologies. The roles of these fungal guilds in deep N cycling must be further studied.

Fungal connectivity

An unexpected finding was the occurrence of numerous, active ERM and ECM taxa at the thaw front. A substantial fraction of

these were designated as potential connectors because they were found in thaw-front soil and on roots in the same profile. ERM taxa along with other RAF ascomycetes are thought to have non-strand-forming mycelia that do not extend far from colonized fine roots (Smith & Read, 2008). Active ERM and other RAF were observed at the thaw front up to 60 cm beyond the roots. These findings contrast with the current paradigm that ericoid roots and ERM activity are constrained to the upper soil layers (Read, 1991). It is, however, important to acknowledge that we do not know whether connector taxa on roots and at the thaw front are from the same fungal genet (sensu Grelet *et al.*, 2010). Furthermore, our predictions that ECM hosts, such as *Betula nana*, would show greater connection to the thaw front than ERM hosts given the traits of the fungi they support, like rhizomorph-forming exploration types (Agerer, 2001), was not supported; instead, all of the hosts examined, ERM in addition to ECM, had RAF that also were observed below roots at the thaw boundary. The origin of these fungi, however, is unknown. Connector fungi may have grown to the thaw front from roots or they may have emerged from thawed permafrost (Pither & Pickles, 2017).

The most abundant connector taxa, such as *Rhizoscyphus* and *Russula* are some of the most frequently observed genera in the Arctic (Timling & Taylor, 2012). Thus, dominant Arctic taxa may play important roles in deep N cycling and plant nutrition. Surprisingly, many of the indicator taxa observed in the present study comprised a miniscule fraction of the overall relative abundance, which may suggest a role for relatively rare taxa in deep N access, too. The environmental variables that structured connector communities observed on root tips also have been implicated in structuring fungal communities across the Arctic (i.e. vegetation composition and SOM characteristics; Timling *et al.*, 2014), suggesting that community patterns through the depth profile may mirror larger geographical patterns. While the correlation between thaw depth and the variation in connector composition at the thaw front suggests that fungal communities vary vertically, even quite deep in the profile.

Permafrost N uptake and fungi

Perhaps the most interesting finding was the occurrence of taxon-specific correlations between the RAF connectivity index and isotope acquisition. The basidiomycete operational taxonomic units (OTUs) with the strongest positive correlations to isotope uptake spanned several genera: *Tylospora*, *Tricholoma*, *Cortinarius*, *Serendipita* and *Lactarius*; while the ascomyceteous fungi covered several guild assignments (DSE, ERM, ECM and multiple guild assignments) and were in the genera *Rhizoscyphus*, *Phialocephala*, *Lachnum* and several helotialian fungi identified at coarser resolution. The abundant *Rhizoscyphus ericae* aggregate showed variable but mostly positive relationships to deep N uptake. Our field observations, therefore, support findings from a controlled experimental setting that show helotialian fungi to be important to plant N uptake (Grelet *et al.*, 2009).

Our finding of both positive and negative correlations between particular RAF connector taxa and tracer acquisition was
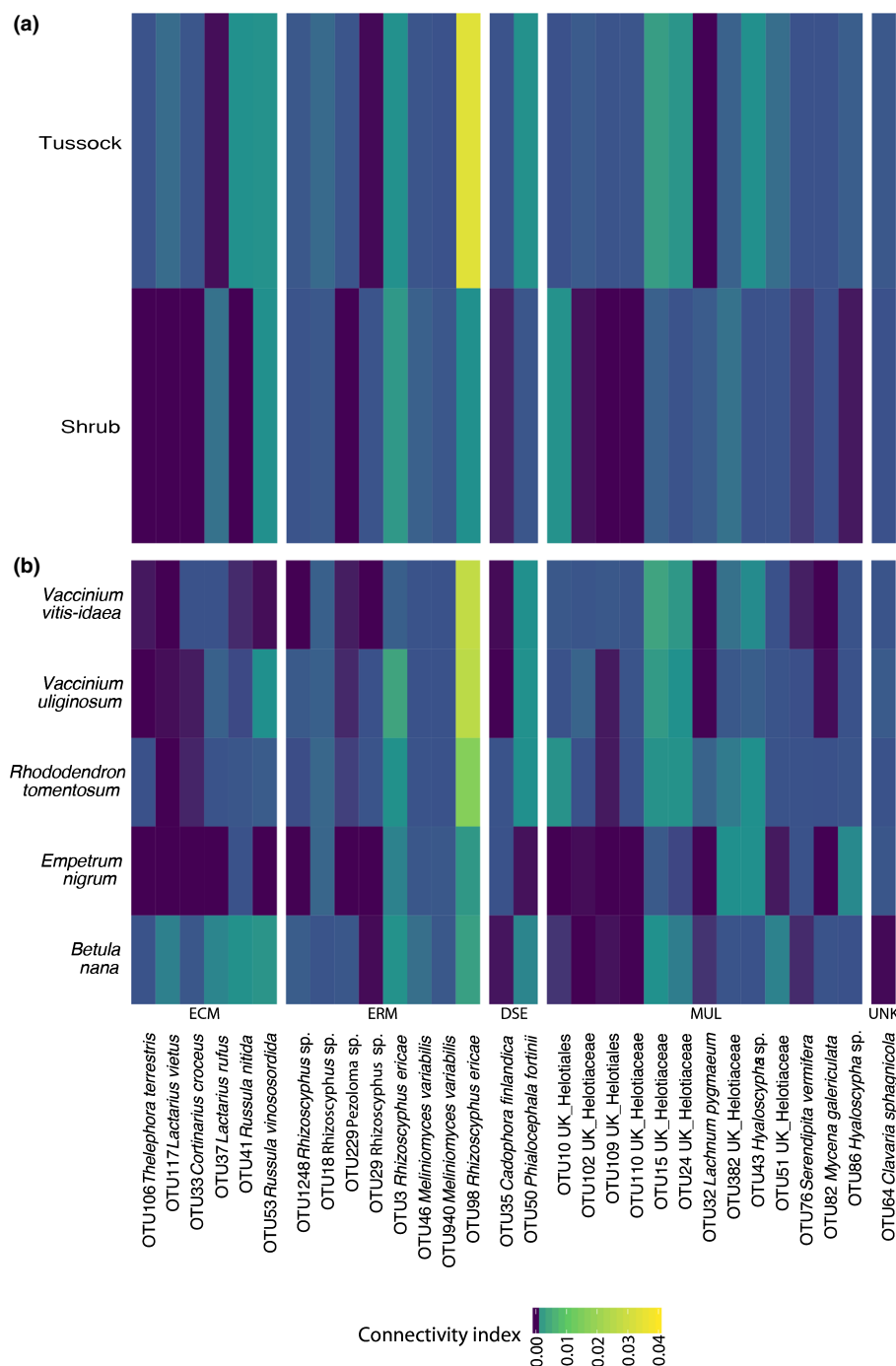
Fig. 6 Putatively root-associated fungal taxa with the highest connectivity between roots and the thaw front by (a) tundra community and (b) host plant species. The fungal connectivity index is calculated from the root-associated fungi connector community (CON$_{TF}$ and CON$_R$) by multiplying the relative abundance of each operational taxonomic unit (OTU) in a root sample by the relative abundance of that OTU in the soil thaw-front sample from that plot. ECM, ectomycorrhizal; ERM, ericoid mycorrhizal; DSE, dark septate endophytes; MUL, multiple guilds; UNK, unassigned due to unknown guild.

unexpected but may help explain why overall connectivity was only modestly related to tracer recovery. One possible explanation for negative correlations between particular OTUs and tracer uptake is that these taxa act more as pathogens or decomposers than as mycorrhizal symbionts, and therefore may be indicators of less healthy roots that would be unlikely to take up tracer. This is supported by the negative or mixed correlations with isotope acquisition by taxa identified in the genera *Serendipita*, *Clavaria*, *Pezoloma*, *Hyaloscypha* and *Mycena*. These taxa all have complex and poorly understood ecologies, and several are closely related to decomposers or pathogens (Birkebak *et al.*, 2013; Weiß *et al.*,

2016; Grelet *et al.*, 2017; Nilsson *et al.*, 2018; Fehrer *et al.*, 2019). We also expect that with more extensive documentation of RAF at the thaw front, greater connectivity would be observed. In this study we conducted limited sampling of roots above and soil near the point of tracer application. As a consequence, it is certain that many fungal species which took up tracer were not, by chance, among the connector OTUs recovered in our soil samples. Furthermore, fungi that were present at the thaw front might have been connected to roots that were not immediately above, and so were not included in our root samples. Despite these factors expected to dilute any signal of tracer movement
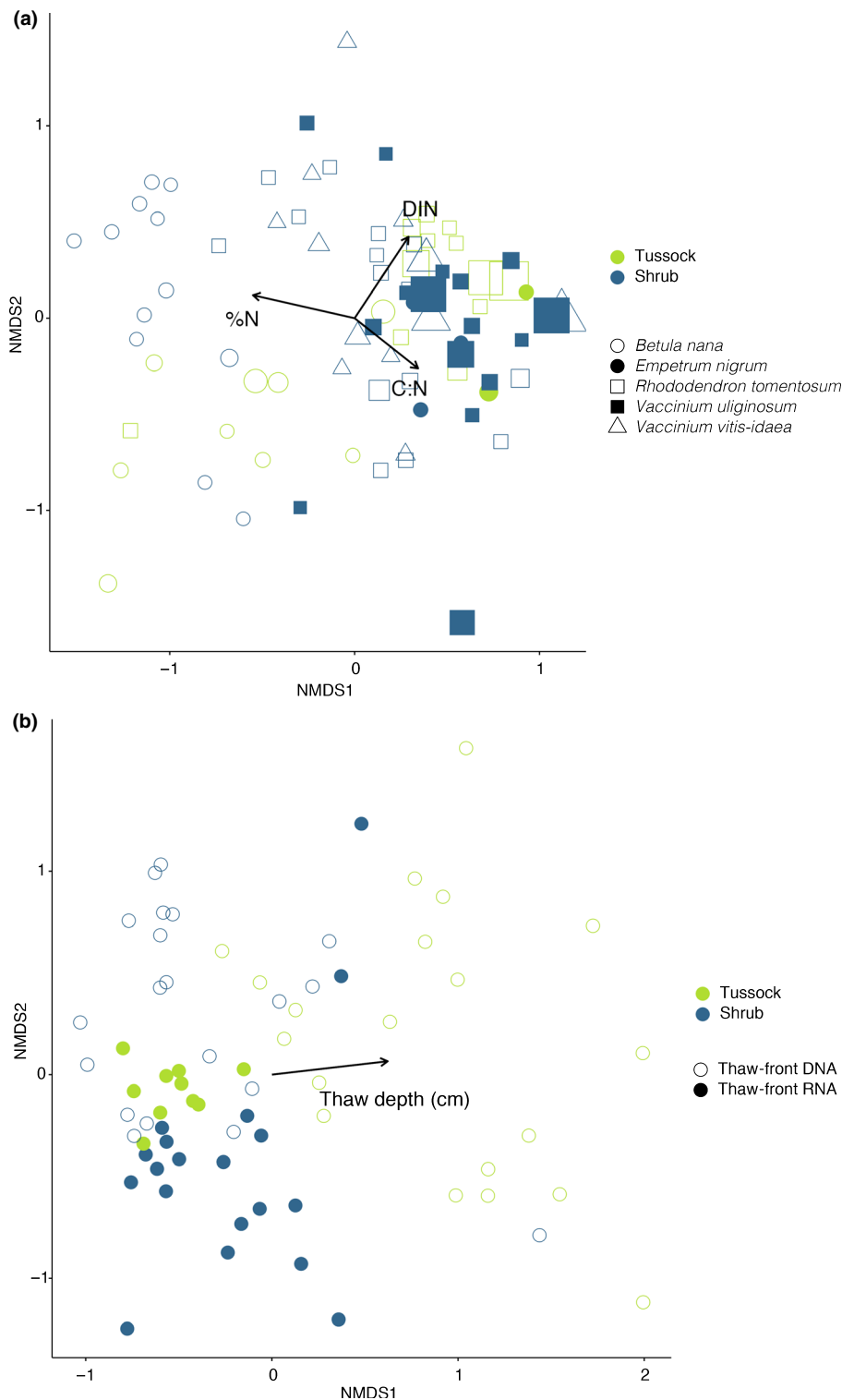
Fig. 7 Correlations between environmental factors and (a) root and (b) thaw-front root-associated fungal connector communities (CON_{TF} and CON_R). (a) Shows the first two axes of the 3D NMDS of the root RAF connector community (CON_R, stress = 0.16, nonmetric fit $R^2 = 0.97$, linear fit $R^2 = 0.84$). The input matrix was 81 samples by 164 taxa. (b) Shows the two axes of the 2D NMDS of the thaw front RAF connector community (CON_{TF}, stress = 0.21, nonmetric fit $R^2 = 0.96$, linear fit $R^2 = 0.83$). The input matrix was 69 samples by 164 taxa. Environmental variables with a correlation P-value < 0.05 were plotted on the NMDS biplots. DIN, dissolved inorganic nitrogen (µg $NO_3 + NH_4$/ode); bulk soil %N by mass, bulk soil C : N; thaw depth (cm), maximum thaw depth per plot.

through connector fungi, we did document significant correlations between individual taxa and isotope recovery and a weaker trend in which the plants with the greatest connectivity also showed the greatest isotope recovery, implicating RAF in the acquisition of thaw front N. Follow-up studies are necessary to directly test causality of the fungal connector taxa in the provision of deep N to plants. One approach might be to sever the fungal connection below the maximum rooting depth of each plant species and measure tracer recovery in plant tissues.

Role of connectors in N cycling

Uptake of permafrost-derived N by fungi could influence local N cycling and ecosystem feedbacks to climate in two main ways.

First, acquisition of newly thawed permafrost-derived N by fungi, regardless of whether it is immediately transferred to plants, would reduce the amount of N lost by hydrological flow or transformations resulting in gaseous loss (Storer *et al.*, 2018). Second, the stimulation of both fungal and plant productivity should sequester C (Clemmensen *et al.*, 2006; Wallander, 2006) and offset some C losses from permafrost soils as they warm.

Fungal biomass and extramatrical mycelium production increases with warming and fertilization (Clemmensen *et al.*, 2006) and thus may provide a sink for permafrost-derived N. Both ECM and ERM production dynamics are largely unknown, particularly in tundra ecosystems or at depths deeper than 10 cm. However, based on estimates of net primary production (NPP) in tussock ($430 \, \text{g m}^{-2} \, \text{yr}^{-1}$) and shrub ($780 \, \text{g m}^{-2} \, \text{yr}^{-1}$) tundra (Shaver, 2013) and estimates of extramatrical mycelium production in relation to NPP (7.2% total NPP; Hobbie, 2006; Ekblad *et al.*, 2013), we would expect $30.96 \, \text{g m}^{-2} \, \text{yr}^{-1}$ in tussock to $56.16 \, \text{g m}^{-2} \, \text{year}^{-1}$ in shrub tundra in extramatrical mycelium production. The N requirement of deciduous plant functional types ranges from 0.60 (tussock) to 4.07 (shrub) and is $0.62 \, \text{g N m}^{-2} \, \text{yr}^{-1}$ for evergreen shrubs (tussock) (Shaver & Chapin, 1991). Fungal requirement ranges from 0.07 to $8.42 \, \text{g N m}^{-2} \, \text{yr}^{-1}$ assuming the aforementioned production and 0.23–15 %N in fungal biomass (Zhang & Elser, 2017). Fungal N demand is rarely considered, but the range of N demand by fungi overlaps substantially with the range of N demand for plants.

The high sink strength of fungi for N could affect long-term patterns of N cycling depending on the turnover of fungal biomass. Although mycelial turnover is rapid in laboratory and mesocosm studies (Bending & Read, 1995; Donnelly *et al.*, 2004; Smith & Read 2008), there are few estimates of fungal biomass turnover in the field. One study estimated boreal forest fungal biomass turnover rate at $0.1 \, \text{yr}^{-1}$ (Wallander *et al.*, 2004; Ekblad *et al.*, 2013), which is similar or slower than root turnover estimates ($0.058–0.958 \, \text{yr}^{-1}$) for tundra and heath (Gill & Jackson, 2000) and suggests a mean residence time of 10 yr (Ekblad *et al.*, 2013). Fungal taxa and guilds also vary in turnover dynamics. Long-distance rhizomorph-forming ECM taxa are associated with rapid mobilization of N and low C sequestration in surface soils, whereas ericoid dominance, with slow growing, slow degrading, melanized hyphae, are associated with high C sequestration (Clemmensen *et al.*, 2015). In our study, upwards of 75% of the relative abundance of thaw-front fungi were ascomycetes including over 300 helotialian OTUs, which may therefore represent a strong sink for permafrost-derived N with a relatively long residence time.

Furthermore, taxon-specific physiological traits of RAF may be an important modulator of plant acquisition of permafrost-derived N. Although controls over N utilization, storage and transfer to hosts by RAF are poorly understood, resource availability and demand are important factors (Näsholm *et al.*, 2013). With the progressive thaw of permafrost soils, N may be held in mycobiont biomass and transferred to host plants over varying timescales. In a companion study, we observed a lag in allocation to foliar tissue by mycorrhizal compared to nonmycorrhizal host

plants (Hewitt *et al.*, 2018). The ability of some fungal taxa to persist beyond the end of the growing season (Tibbett & Cairney, 2007) could result in fungal uptake of permafrost-derived N late in the growing season when the active layer is deepest, winter sequestration, and, for RAF, a lag in transfer to plant parts until sink strength increases during the following growing season.

The stimulation of plant productivity due to deep N uptake has been demonstrated for deeply rooted nonmycorrhizal plants (Keuper *et al.*, 2017), but has yet to be shown for ERM and ECM shrubs. Importantly, these are the plants most likely to provide a C offset against permafrost C emissions as these ecosystems warm due to their longer tissue residence times. Although the drivers of competitive (fungal acquisition without deep N transfer to plant hosts) vs facilitative (transfer of deep N to plant hosts) interactions between tundra shrubs and mycobionts have yet to be fully elucidated, our results demonstrate fungal uptake of deep N and suggest that fungal allocation of permafrost nutrients is critical to predicting the effects of deep N release on tundra ecosystem N and C cycling.

Author contributions

MCM and REH designed the field experiment; REH conducted fieldwork and isotope analysis, and drafted the manuscript; DLT, IVL and MRD conducted molecular verification of root identities, fungal sequencing and bioinformatics; HG corrected root IDs for final analysis; REH, MRD and DLT analyzed the data; REH, MRD, IVL, HG, ADM, DLT and MCM made contributions to manuscript revision.

ORCID

M. Rae DeVan (iD) https://orcid.org/0000-0002-4955-4181
Helene Genet (iD) https://orcid.org/0000-0003-4537-9563
Rebecca E. Hewitt (iD) https://orcid.org/0000-0002-6668-8472
Michelle C. Mack (iD) https://orcid.org/0000-0003-1279-4242
A. David McGuire (iD) https://orcid.org/0000-0003-4646-0750
D. Lee Taylor (iD) https://orcid.org/0000-0002-5985-9210

References

Agerer R. 2001. Exploration types of ectomycorrhizae – a proposal to classify ectomycorrhizal mycelial systems according to their patterns of differentiation and putative ecological importance. *Mycorrhiza* 11: 107–114.

Bates D, Mächler M, Bolker B, Walker S. 2015. Fitting linear mixed-effects models using lme4. *Journal of Statistical Software* 67: doi: 10.18637/jss.v067.i01.

Bending GD, Read DJ. 1995. The structure and function of the vegetative mycelium of ectomycorrhizal plants: foraging behavior and translocation of nutrients from exploited litter. *New Phytologist* 130: 401–409.

Bending GD, Read DJ. 1996. Nitrogen mobilization from protein-polyphenol complex by ericoid and ectomycorrhizal fungi. *Soil Biology & Biochemistry* 28: 1603–1612.

Bergemann SE, Miller SL. 2002. Size, distribution, and persistence of genets in local populations of the late-stage ectomycorrhizal basidiomycete, *Russula brevipes*. *New Phytologist* 156: 313–320.

Birkebak JM, Mayor JR, Ryberg KM, Matheny PB. 2013. A systematic, morphological and ecological overview of the Clavariaceae (Agaricales). *Mycologia* 105: 896–911.

Biskaborn BK, Smith SL, Noetzli J, Matthes H, Vieira G, Streletskiy DA, Schoeneich P, Romanovsky VE, Lewkowicz AG, Abramov A *et al.* 2019. Permafrost is warming at a global scale. *Nature Communications* 10: 264–264.

Blume-Werry G, Milbau A, Teuber LM, Johansson M, Dorrepaal E. 2019. Dwelling in the deep – strongly increased root growth and rooting depth enhance plant interactions with thawing permafrost soil. *New Phytologist* 223: 1328–1339.

Bonello P, Bruns TD, Gardes M. 1998. Genetic structure of a natural population of the ectomycorrhizal fungus *Suillus pungens*. *New Phytologist* 138: 533–542.

Burnham KP, Anderson DR. 2002. *Model selection and multimodel inference: a practical information-theoretic approach*. New York: Springer.

Chapin FS III, Shaver GR, Giblin AE, Nadelhoffer KG, Laundre JA. 1995. Response of arctic tundra to experimental and observed changes in climate. *Ecology* 76: 694–711.

Clemmensen KE, Finlay RD, Dahlberg A, Stenlid J, Wardle DA, Lindahl BD. 2015. Carbon sequestration is related to mycorrhizal fungal community shifts during long-term succession in boreal forests. *New Phytologist* 205: 1525–1536.

Clemmensen KE, Michelsen A, Jonasson S, Shaver GR. 2006. Increased ectomycorrhizal fungal abundance after long-term fertilization and warming of two arctic tundra ecosystems. *New Phytologist* 171: 391–404.

Dahlberg A, Stenlid J. 1990. Population structure and dynamics in *Suillus bovinus* as indicated by spatial distribution of fungal clones. *New Phytologist* 115: 487–493.

De Caceres M, Legendre P. 2009. Associations between species and groups of sites: indices and statistical inference. *Ecology* 90: 3566–3574.

Deshpande V, Wang Q, Greenfield P, Charleston M, Porras-Alfaro A, Kuske CR, Cole JR, Midgley DJ, Tran-Dinh N. 2016. Fungal identification using a Bayesian classifier and the Warcup training set of internal transcribed spacer sequences. *Mycologia* 108: 1–5.

DeMarco J, Mack MC, Bret-Harte MS. 2014. Effects of arctic shrub expansion on biophysical vs. biogeochemical drivers of litter decomposition. *Ecology* 95: 1861–1875.

Dickie IA, Koide RT, Stevens CM. 1998. Tissue density and growth response of ectomycorrhizal fungi to nitrogen source and concentration. *Mycorrhiza* 8: 145–148.

Dighton J. 2007. Nutrient cycling by saprotrophic fungi in terrestrial habitats. In: Kubicek C, Druzhinina IS, eds. *Environmental and microbial relationships. The Mycota*. Berlin, Germany: Springer, 287–300.

Donnelly DP, Boddy L, Leake JR. 2004. Development, persistence and regeneration of foraging ectomycorrhizal mycelial systems in soil microcosms. *Mycorrhiza* 14: 37–45.

Edgar RC. 2013. UPARSE: highly accurate OTU sequences from microbial amplicon reads. *Nature Methods* 10: 996–998.

Ekblad A, Wallander H, Godbold DL, Cruz C, Johnson D, Baldrian P, Björk RG, Epron D, Kieliszewska-Rokicka B, Kjøller R *et al.* 2013. The production and turnover of extramatrical mycelium of ectomycorrhizal fungi in forest soils: role in carbon cycling. *Plant and Soil* 366: 1–27.

Elmendorf SC, Henry GHR, Hollister RD, Bjork RG, Boulanger-Lapointe N, Cooper EJ, Cornelissen JHC, Day TA, Dorrepaal E, Elumeeva TG *et al.* 2012. Plot-scale evidence of tundra vegetation change and links to recent summer warming. *Nature Climate Change* 2: 453–457.

Fehrer J, Réblová M, Bambasová V, Vohník M. 2019. The root-symbiotic *Rhizoscyphus ericae* aggregate and *Hyaloscypha* (Leotiomycetes) are congeneric: Phylogenetic and experimental evidence. *Studies in Mycology* 92: 195–225.

Gill RA, Jackson RB. 2000. Global patterns of root turnover for terrestrial ecosystems. *New Phytologist* 147: 13–31.

Grelet GA, Ba R, Goeke DF, Houliston GJ, Taylor AFS, Durall DM. 2017. A plant growth-promoting symbiosis between *Mycena galopus* and *Vaccinium corymbosum* seedlings. *Mycorrhiza* 27: 831–839.

Grelet GA, Johnson D, Vralstad T, Alexander IJ, Anderson IC. 2010. New insights into the mycorrhizal *Rhizoscyphus ericae* aggregate: spatial structure and co-colonization of ectomycorrhizal and ericoid roots. *New Phytologist* 188: 210–222.

Grelet GA, Meharg AA, Duff EI, Anderson IC, Alexander IJ. 2009. Small genetic differences between ericoid mycorrhizal fungi affect nitrogen uptake by *Vaccinium*. *New Phytologist* 181: 708–718.

Hewitt RE, Taylor DL, Genet H, McGuire AD, Mack MC. 2018. Below-ground plant traits influence tundra plant acquisition of newly thawed permafrost nitrogen. *Journal of Ecology* 107: 1–13.

Hobbie EA. 2006. Carbon allocation to ectomycorrhizal fungi correlates with belowground allocation in culture studies. *Ecology* 87: 563–569.

Hobbie EA, Horton TR. 2007. Evidence that saprotrophic fungi mobilise carbon and mycorrhizal fungi mobilise nitrogen during litter decomposition. *New Phytologist* 173: 447–449.

Hogberg MN, Chen Y, Hogberg P. 2007. Gross nitrogen mineralisation and fungi-to-bacteria ratios are negatively correlated in boreal forests. *Biology and Fertility of Soils* 44: 363–366.

Jorgenson JC, Raynolds MK, Reynolds JH, Benson A-M. 2015. Twenty-five year record of changes in plant cover on tundra of Northeastern Alaska. *Arctic, Antarctic, and Alpine Research* 47: 785–806.

Keuper F, van Bodegom PM, Dorrepaal E, Weedon JT, van Hal J, van Logtestijn RSP, Aerts R. 2012. A frozen feast: thawing permafrost increases plant-available nitrogen in subarctic peatlands. *Global Change Biology* 18: 1998–2007.

Keuper F, Dorrepaal E, van Bodegom PM, van Logtestijn R, Venhuizen G, van Hal J, Aerts R. 2017. Experimentally increased nutrient availability at the permafrost thaw front selectively enhances biomass production of deep-rooting subarctic peatland species. *Global Change Biology* 23: 4257–4266.

Kruskal JB. 1964. Nonmetric multidimensional scaling: a numerical method. *Psychometrika* 29: 115–129.

Mack MC, Finlay JC, DeMarco J, Chapin FS III, Schuur AEG, Neff JC, Zimov SA. 2010. *Nitrogen and phosphorus in Yedoma soils of Northeast Siberia: stocks, fluxes and the ecosystem consequences of nutrient release from permafrost thaw*. Fall Meeting AGU, San Francisco, CA, USA, 13–17 December 2010. [WWW document] URL https://ui.adsabs.harvard.edu/abs/2010AGUFMGC52A..05M/abstract [accessed 21 April 2019].

Mack MC, Schuur EAG, Bret-Harte MS, Shaver GR, Chapin FS. 2004. Ecosystem carbon storage in arctic tundra reduced by long-term nutrient fertilization. *Nature* 431: 440–443.

Martin AC, Jeffers ES, Petrokofsky G, Myers-Smith I, Macias-Fauria M. 2017. Shrub growth and expansion in the Arctic tundra: an assessment of controlling factors using an evidence-based approach. *Environmental Research Letters* 12: 085007.

Mauritz M, Bracho R, Celis G, Hutchings J, Natali SM, Pegoraro E, Salmon VG, Schädel C, Webb EE, Schuur EAG. 2017. Nonlinear CO_2 flux response to 7 years of experimentally induced permafrost thaw. *Global Change Biology* 23: 3646–3666.

Mazerolle MJ. 2019. *AICcmodavg: Model selection and multimodel inference based on (Q)AIC(c). R package v.2.2-2*. [WWW document] URL https://cran.r-project.org/package=AICcmodavg [accessed 9 October 2017]

McMurdie PJ, Holmes S. 2013. phyloseq: an R package for reproducible interactive analysis and graphics of microbiome census data. *PLoS ONE* 8: e61217.

Myers-Smith IH, Forbes BC, Wilmking M, Hallinger M, Lantz T, Blok D, Tape KD, Macias-Fauria M, Sass-Klaassen U, Levesque E *et al.* 2011. Shrub expansion in tundra ecosystems: dynamics, impacts and research priorities. *Environmental Research Letters* 6: 045509.

Näsholm T, Högberg P, Franklin O, Metcalfe D, Keel SG, Campbell C, Hurry V, Linder S, Högberg MN. 2013. Are ectomycorrhizal fungi alleviating or aggravating nitrogen limitation of tree growth in boreal forests? *New Phytologist* 198: 214–221.

Newsham KK. 2011. A meta-analysis of plant responses to dark septate root endophytes. *New Phytologist* 190: 783–793.

Newsham KK, Upson R, Read DJ. 2009. Mycorrhizas and dark septate root endophytes in polar regions. *Fungal Ecology* 2: 10–20.

Nguyen NH, Song Z, Bates ST, Branco S, Tedersoo L, Menke J, Schilling JS, Kennedy PG. 2016. FUNGuild: An open annotation tool for parsing fungal community datasets by ecological guild. *Fungal Ecology* 20: 241–248.

Nilsson RH, Larsson K-H, Taylor AFS, Bengtsson-Palme J, Jeppesen TS, Schigel D, Kennedy P, Picard K, Glöckner FO, Tedersoo L *et al*. 2018. The UNITE database for molecular identification of fungi: handling dark taxa and parallel taxonomic classifications. *Nucleic Acids Research* 47: D259–D264.

Oksanen J, Blanchet FG, Kindt R, Legendre P, Minchin PR, O'Hara R, Simpson GL, Solymos P, Stevens MHH, Wagner H. 2012. *vegan: community ecology packag, v.2.5-4 2(9)*. [WWW document] URL https://CRAN.R-project.org/package=vegan [accessed 8 February 2018].

Osterkamp TE, Romanovsky VE. 1999. Evidence for warming and thawing of discontinuous permafrost in Alaska. *Permafrost and Periglacial Processes* 10: 17–37.

Penton CR, St Louis D, Cole JR, Luo Y, Wu L, Schuur EAG, Zhou J, Tiedje JM. 2013. Fungal diversity in permafrost and tallgrass prairie soils under experimental warming conditions. *Applied and Environmental Microbiology* 79: 7063–7072.

Phillips RP, Brzostek E, Midgley MG. 2013. The mycorrhizal-associated nutrient economy: a new framework for predicting carbon–nutrient couplings in temperate forests. *New Phytologist* 199: 41–51.

Pinheiro J, Bates D, DebRoy S, Sarkar D, R Core Team. 2017. *nlme: Linear and nonlinear mixed effects models: R package v.3.1-131*. [WWW document] URL https://CRAN.R-project.org/package=nlme [accessed 5 July 2019].

Pither J, Pickles BJ. 2017. The paleosymbiosis hypothesis: host plants can be colonised by root symbionts that have been inactive for centuries to millenia. *FEMS Microbiology Ecology* 93.

Plaza C, Pegoraro E, Bracho R, Celis G, Crummer KG, Hutchings JA, Hicks Pries CE, Mauritz M, Natali SM, Salmon VG *et al*. 2019. Direct observation of permafrost degradation and rapid soil carbon loss in tundra. *Nature Geoscience* 12: 627–631.

R Core Team. 2018. *R: A language and environment for statistical computing*. Vienna, Austria: R Foundation for Statistical Computing.

Read DJ. 1991. Mycorrhizas in ecosystems. *Experientia* 47: 376–391.

Read DJ. 1996. The structure and function of the ericoid mycorrhizal root. *Annals of Botany* 77: 365–374.

Read DJ, Perez-Moreno J. 2003. Mycorrhizas and nutrient cycling in ecosystems - a journey towards relevance? *New Phytologist* 157: 475–492.

Rocha AV, Blakely B, Jiang Y, Wright KS, Curasi SR. 2018. Is arctic greening consistent with the ecology of tundra? Lessons from an ecologically informed mass balance model. *Environmental Research Letters* 13: 125007.

Salmon VG, Schädel C, Bracho R, Pegoraro E, Celis G, Mauritz M, Mack MC, Schuur EAG. 2018. Adding depth to our understanding of nitrogen dynamics in permafrost soils. *Journal of Geophysical Research: Biogeosciences* 123: 2497–2512.

Schimel JP, Kielland K, Chapin FS.1996. Nutrient availability and uptake by tundra plants. In: Reynolds JF, Tenhunen JD, eds. *Landscape function and disturbance in arctic tundra*. Berlin, Germany: Springer, 203–221.

Schuur EAG, Bockheim J, Canadell JG, Euskirchen E, Field CB, Goryachkin SV, Hagemann S, Kuhry P, Lafleur PM, Lee H *et al*. 2008. Vulnerability of permafrost carbon to climate change: implications for the global carbon cycle. *BioScience* 58: 701–714.

Schuur EAG, Crummer KG, Vogel JG, Mack MC. 2007. Plant species composition and productivity following permafrost thaw and thermokarst in Alaskan tundra. *Ecosystems* 10: 280–292.

Shaver G. 2013. *NPP Tundra: Toolik Lake, Alaska, 1982*. Oak Ridge, TN, USA: Oak Ridge National Laboratory Distributed Active Archive Center.

Shaver GR, Bret-Harte SM, Jones MH, Johnstone J, Gough L, Laundre J, Chapin FS. 2001. Species composition interacts with fertilizer to control long-term change in tundra productivity. *Ecology* 82: 3163–3181.

Shaver GR, Chapin FS III. 1991. Production:biomass relationships and element cycling in contrasting arctic vegetation types. *Ecological Monographs* 61: 1–31.

Sistla SA, Moore JC, Simpson RT, Gough L, Shaver GR, Schimel JP. 2013. Long-term warming restructures Arctic tundra without changing net soil carbon storage. *Nature* 497: 615–618.

Smith SE, Read DJ. 2008. *Mycorrhizal symbiosis*. New York, NY, USA: Academic Press.

Storer K, Coggan A, Ineson P, Hodge A. 2018. Arbuscular mycorrhizal fungi reduce nitrous oxide emissions from N₂O hotspots. *New Phytologist* 220: 1285–1295.

Tape K, Sturm M, Racine C. 2006. The evidence for shrub expansion in Northern Alaska and the Pan-Arctic. *Global Change Biology* 12: 686–702.

Taylor DL, Walters WA, Lennon NJ, Bochicchio J, Krohn A, Caporaso JG, Pennanen T. 2016. Accurate estimation of fungal diversity and abundance through improved lineage-specific primers optimized for illumina amplicon sequencing. *Applied and Environmental Microbiology* 82: 7217–7226.

Tibbett M. 2000. Roots, foraging and the exploitation of soil nutrient patches: the role of mycorrhizal symbiosis. *Functional Ecology* 14: 397–399.

Tibbett M, Cairney JWG. 2007. The cooler side of mycorrhizas: their occurrence and functioning at low temperatures. *Canadian Journal of Botany* 85: 51–62.

Timling I, Dahlberg A, Walker DA, Gardes M, Charcosset J-Y, Welker JM, Taylor DL. 2012. Distribution and drivers of ectomycorrhizal fungal communities across the North American Arctic. *Ecosphere* 3: 1–25.

Timling I, Taylor DL. 2012. Peeking through a frosty window: molecular insights into the ecology of Arctic soil fungi. *Fungal Ecology* 5: 419–429.

Timling I, Walker DA, Nusbaum C, Lennon NJ, Taylor DL. 2014. Rich and cold: diversity, distribution and drivers of fungal communities in patterned-ground ecosystems of the North American Arctic. *Molecular Ecology* 23: 3258–3272.

Vogel J, Schuur EAG, Trucco C, Lee H. 2009. Response of CO₂ exchange in a tussock tundra ecosystem to permafrost thaw and thermokarst development. *Journal of Geophysical Research: Biogeosciences* 114: G04018.

Walker JF, Aldrich-Wolfe L, Riffel A, Barbare H, Simpson NB, Trowbridge J, Jumpponen A. 2011. Diverse Helotiales associated with the roots of three species of Arctic Ericaceae provide no evidence for host specificity. *New Phytologist* 191: 515–527.

Wallander H. 2006. External mycorrhizal mycelia: the importance of quantification in natural ecosystems. *New Phytologist* 171: 240–242.

Wallander H, Goransson H, Rosengren U. 2004. Production, standing biomass and natural abundance of ¹⁵N and ¹³C in ectomycorrhizal mycelia collected at different soil depths in two forest types. *Oecologia* 139: 89–97.

Wallenstein MD, McMahon S, Schimel J. 2007. Bacterial and fungal community structure in Arctic tundra tussock and shrub soils. *FEMS Microbiology Ecology* 59: 428–435.

Weigt RB, Raidl S, Verma R, Agerer R. 2012. Exploration type-specific standard values of extramatrical mycelium—a step towards quantifying ectomycorrhizal space occupation and biomass in natural soil. *Mycological Progress* 11: 287–297.

Weiß M, Waller F, Zuccaro A, Selosse M-A. 2016. Sebacinales – one thousand and one interactions with land plants. *New Phytologist* 211: 20–40.

Zhang J, Elser JJ. 2017. Carbon : nitrogen : phosphorus stoichiometry in fungi: a meta-analysis. *Frontiers in Microbiology* 8: 1281–1281.

Zuur A, Ieno E, Walker N, Saveliev A, Smith G. 2009. *Mixed effects models and extensions in ecology*. New York, NY, USA: Springer.

Supporting Information

Additional Supporting Information may be found online in the Supporting Information section at the end of the article.

Fig. S1 Family- to genus-level ITS maximum-likelihood trees constructed to improve the identification of selected poorly resolved fungal operational taxonomic units observed at the permafrost thaw front or on the roots of ectomycorrhizal and ericoid mycorrhizal shrubs in tussock and shrub tundra near Eight Mile Lake, AK, USA.

Fig. S2 Conceptual diagram of fungal community subsets from permafrost thaw-front and root communities.

Fig. S3 Putatively root-associated fungal connectivity between roots and the thaw-front environment for each host species in tussock and shrub tundra in relation to (a) fine root: thaw depth (1 = at the thaw front, 0 indicates the surface of the soil profile) and (b) fine-root biomass (g m^{-2}).

Fig. S4 NMDS ordination of root and thaw front soil root-associated fungal communities (RAF$_R$ + RAF$_{TF}$) in tussock and shrub tundra at Eight Mile Lake, AK, USA.

Methods S1 Field and laboratory methods for biogeochemical datasets and characterizing root and thaw-front fungal communities in tussock and shrub tundra at Eight Mile Lake, AK, USA.

Table S1 Fungal operational taxonomic units observed in root DNA and thaw front soil RNA and DNA profiles at Eight Mile Lake, AK, USA.

Table S2 Subsets of the observed fungal communities at the thaw front and on root systems of mycorrhizal host plants at Eight Mile Lake, AK, USA.

Table S3 Correlation coefficients between OTU-level connectivity index and fine-root ^{15}N isotope pool (g m^{-2}) or overall percentage tracer recovered.

Table S4 Correlation coefficients between environmental variables and NMDS ordinations of connector fungal composition observed in root and thaw front soil RNA and DNA profiles at Eight Mile Lake, AK, USA.

Please note: Wiley Blackwell are not responsible for the content or functionality of any Supporting Information supplied by the authors. Any queries (other than missing material) should be directed to the *New Phytologist* Central Office.

About *New Phytologist*

- *New Phytologist* is an electronic (online-only) journal owned by the New Phytologist Trust, a **not-for-profit organization** dedicated to the promotion of plant science, facilitating projects from symposia to free access for our Tansley reviews and Tansley insights.

- Regular papers, Letters, Research reviews, Rapid reports and both Modelling/Theory and Methods papers are encouraged. We are committed to rapid processing, from online submission through to publication 'as ready' via *Early View* – our average time to decision is <26 days. There are **no page or colour charges** and a PDF version will be provided for each article.

- The journal is available online at Wiley Online Library. Visit **www.newphytologist.com** to search the articles and register for table of contents email alerts.

- If you have any questions, do get in touch with Central Office (np-centraloffice@lancaster.ac.uk) or, if it is more convenient, our USA Office (np-usaoffice@lancaster.ac.uk)

- For submission instructions, subscription and all the latest information visit **www.newphytologist.com**